Original Article

Journal of Tissue Engineering
Volume 5: 1–10

DOI: 10.1177/2041731414552114
tej.sagepub.com
SAGE

Scanning electron microscopical observation of an osteoblast/osteoclast co-culture on micropatterned orthopaedic ceramics

Mansur Halai[1,2], Andrew Ker[1,2], RM Dominic Meek[2], Danish Nadeem[3], Terje Sjostrom[3], Bo Su[3], Laura E McNamara[1], Matthew J Dalby[1] and Peter S Young[1]

Abstract

In biomaterial engineering, the surface of an implant can influence cell differentiation, adhesion and affinity towards the implant. On contact with an implant, bone marrow–derived mesenchymal stromal cells demonstrate differentiation towards bone forming osteoblasts, which can improve osteointegration. The process of micropatterning has been shown to improve osteointegration in polymers, but there are few reports surrounding ceramics. The purpose of this study was to establish a co-culture of bone marrow–derived mesenchymal stromal cells with osteoclast progenitor cells and to observe the response to micropatterned zirconia toughened alumina ceramics with 30 µm diameter pits. The aim was to establish whether the pits were specifically bioactive towards osteogenesis or were generally bioactive and would also stimulate osteoclastogenesis that could potentially lead to osteolysis. We demonstrate specific bioactivity of micropatterns towards osteogenesis, with more nodule formation and less osteoclastogenesis compared to planar controls. In addition, we found that that macrophage and osteoclast-like cells did not interact with the pits and formed fewer full-size osteoclast-like cells on the pitted surfaces. This may have a role when designing ceramic orthopaedic implants.

Keywords

Ceramic, micropattern, osteointegration, co-culture

Received: 5 June 2014; accepted: 20 August 2014

Introduction

Osteointegration, which is defined as a combination of the structural and functional affinities between living bone and the surface of a load-bearing implant, is essential for implant-host survival and thus implant longevity.[1] Osteoblasts are the key bone forming cells in the human body involved in osteointegration. They are derived from bone marrow–derived mesenchymal stromal cells (BMSC), which can differentiate towards cells of the osteoblastic, chondrogenic, reticular or adipocytic lineages.[2] It is important that BMSC differentiate towards osteoblastic progenitors when in contact with an orthopaedic implant that has been introduced into the body, in order to initiate new bone formation rather than the more commonly seen soft tissue encapsulation.[3] This encapsulation can potentially result in implant failure, by inducing loosening.[4] New bone is subsequently maintained through bone remodelling, regulated by

[1]Centre for Cell Engineering, Institute of Molecular, Cell and Systems Biology, University of Glasgow, Glasgow, UK
[2]Department of Orthopaedics, Southern General Hospital, Glasgow, UK
[3]School of Oral and Dental Sciences, University of Bristol, Bristol, UK

Corresponding author:
Mansur Halai, Centre for Cell Engineering, Institute of Molecular, Cell and Systems Biology, University of Glasgow, Joseph Black Building, Glasgow G12 8QQ, UK.
Email: mansurhalai@hotmail.com

continuous cycles of bone resorption and formation. In vivo, there is a complex interaction between bone forming osteoblasts and bone resorbing osteoclasts, which are derived from bone marrow–derived haematopoietic cells (BMHC).[5] The interplay between these two cell types is vitally important for normal bone homeostasis. It would be theoretically beneficial for an implant interface to be able to control osteoclast differentiation and activity, limiting bone resorption without significantly limiting normal bone remodelling responsible for removing bone. In other words, we require implants that are specifically bioactive (osteoinductive) and not generally bioactive (increasing bone formation and osteolysis).

Ceramic materials are being introduced into the biomaterials industry at a growing rate due to their improved fracture resistance, high strength, low wear properties and excellent biocompatibility.[6] Their use in total hip arthroplasty, predominately as a bearing surface, has increased the interest in this material. Ceramics, such as alumina or zirconia toughened alumina (ZTA), are being used as small joint replacements where the bone makes direct contact with the ceramic.[7] Due to their inherent bioinertness, osteointegration into ceramics tends to be poor. Techniques such as sand-blasting and etching, which are used to surface roughen titanium and metal alloys to increase osteointegration, are not practical with brittle ceramics.[8] Cells react to their environment and the shape of their environment is influential to this reaction.[9] The recent literature has demonstrated that surface topography can alter cell behavior.[10,11] Microtopography on certain materials has been shown to induce cell adhesion, cell migration and genetic changes within the cells.[12,13] Therefore, it would be desirable to achieve some form of topographical modification in ceramics.

Microfabrication techniques have been demonstrated to create precise micropatterns to the topography of silicones and polymer materials.[14] One report that has used microfabrication techniques, demonstrated that surface topographic features on polymers, from submicron to micron-scales (up to 50 μm), produced large changes in response from protein adsorption and BMSC on these polymeric surfaces.[15] Subsequent reports have noted that pitted features with a diameter of 30–40 μm have had osteogenic effects when imprinted in polymethylmethacrylate, polycaprolactone or fibrous hydrogels.[16,17] The presence of micropatterns on ceramic materials could thus, theoretically, improve osteointegration.[18] In vitro stem cell co-cultures allow observation of the complex interactions between BMSC and BMHC and provide the most accurate model for assessing biomaterials and their effect on both bone formation and normal bone turnover.[19] Several authors report successful co-cultures of osteoblast cell lines or primary osteoblasts combined with peripheral blood mononuclear cells (PBMC) or isolated monocytes, usually of murine or human origin, cultivated with the addition of macrophage colony-stimulating factor (M-CSF).[20–22] Previously, the authors have reported co-cultures based on BMSC. Nakagawa et al. used porcine BMSC and BMHC, and Heinemann et al. studied human BMSC and human PBMC.[23–25] However, none of these previously described co-cultures utilised human BMHC and human BMSC without supplementation with, for example, M-CSF. Such a culture using human cells, free from supplementation, would most closely represent the in vivo environment. Supplementation to encourage either osteoblast or osteoclast differentiation will affect differentiation and activity of the other cell lines, potentially affecting study outcomes.[26]

In order to evaluate the effects of altering the surface properties on the adhesion and interaction of cells involved in osteointegration and bone remodelling, we have developed a unique co-culture of human BMSC and BMHC. We aimed to observe development of the co-culture on ZTA ceramic materials and to provide a qualitative evaluation of the micropatterning effect on ZTA ceramic surfaces with 30 μm diameter pits.

Materials and methods

Micropatterning of ceramics

Nickel (Ni) masks with a micropattern of 40 μm diameter pillars were fabricated using a standard photolithography and electroplating technique.[27] Briefly, micropatterns were fabricated into silicon wafers through a conventional photolithography process, which included photo masking, exposure and development procedures. An electroforming process was then used to fabricate the Ni metal mask of 50 × 50 mm on the patterned substrate. The Ni mask was then separated from the substrate after the Ni deposit thickness reached >100 μm. Micropatterned ceramic substrates were produced by embossing of visco-plastic green ceramic tapes at room temperature followed by sintering. Green ceramic tapes were fabricated using a viscous polymer process (VPP) as described before.[28] Briefly, 90 wt% alumina powder (CT3000SG; Almatis, USA) with an average particle size of 0.5 μm and 10 wt% zirconia (Tosoh TZ-3YS-E, Japan) with an average particle size of 0.6 μm were mixed with a polymer binder, polyvinyl butyral (PVB, Dow Chemicals, USA), with cyclohexanone (Sigma–Aldrich, UK) as a solvent. Premixed ceramic powder and polymer binder/solvent were milled under high shear stress on a twin-roll mill (Winkworth Machinery, UK) for 10–15 min to form a visco-plastic dough. Green ceramic tapes were obtained by calendering. Embossing was carried out on 50 × 50 mm^2 of green ceramic tape using a mechanical testing machine (Z020; Zwick Roell, Germany) under controlled pressure and loading rate. Embossing was carried out at 1.5, 3, 4, 5, and 6 MPa, at a rate of 0.05 MPa s^{-1} up to the required pressure. After

drying at 150°C overnight, the micropatterned ceramics were sintered using the following sintering regime (also designed to remove surplus polymer): the temperature was first increased at a heating rate of 1°C/min, to 600°C with a duration of 2 h, followed by a further increase in temperature at a heating rate of 10°C/min, to 1600°C with a duration of 2 h.

BMSC/BMHC isolation

After informed consent was obtained from healthy patients undergoing routine total hip arthroplasty, bone marrow was aspirated from the femoral medullary canal. This was stored for transfer in a medium of phosphate-buffered saline (PBS), 0.53 mM ethylenediaminetetraacetic acid (EDTA), and antibiotics (6.74 U mL^{-1} Penicillin–Streptomycin, 0.2 μg mL^{-1} Fungizone). The bone marrow aspirate was washed with Modified Dulbecco's Modified Eagle's Medium (mDMEM; DMEM (D5671), 10% foetal bovine serum, 100 mM sodium pyruvate, 200 mM L-glutamine (Invitrogen, UK), and antibiotics. It was then centrifuged at 376 g for 10 min, repeated twice. The cell pellets were resuspended in mDMEM and overlaid on a Ficoll gradient. This was then centrifuged at 445 g for 45 min and the subsequent mononuclear interface layer aspirated and resuspended in mDMEM. The cells were further washed as previously and finally plated at a density of 1×10^6 in 25 cm^2 in vented cell culture flasks and incubated at 37°C with 5% humidified CO_2.

BMSC/BMHC co-culture

In brief; at day 3, non-adherent cells were removed within the supernatant and cultured separately as BMHC; the remaining adherent cells were assumed to be BMSCs and were cultured for a further 7–10 days until a confluent BMSC layer was identified. The cells were then detached with 0.05% trypsin/0.53 mM EDTA, centrifuged and resuspended in mDMEM to a concentration of 3×10^4 cells/mL. A 1-mL amount of cell suspension was pipetted directly onto the prepared substrates and allowed to settle over 30 min. Thereafter, 3 mL of media was added to the wells, repeated on day 3. At day 7, 1 mL of BMHC suspension was added at a concentration of 1.2×10^5 cells/mL. The co-culture was maintained up to specific time points (days 3, 7, 14, 21 and 28) with thrice weekly media exchange. At each time point, duplicate samples were fixed and prepared for analysis by scanning electron microscopy (SEM). This co-culture method has been recently described and shown to yield successful co-culture of osteoclast and osteoblast lineages without extraneous supplementation.[29]

SEM

Cells were fixed in 4% glutaraldehyde, postfixed in osmium tetroxide, dehydrated through a graded alcohol series and hexamethyldisiloxane (HMDS) and air dried prior to sputter coating (20 nm gold/palladium) and viewing with Zeiss Sigma FE-SEM.

Histochemical staining

After 28 days of co-culture, cells were fixed (4% formaldehyde for 30 s and stained for tartrate-resistant acid phosphatase (TRAP) as per manufacturer's instructions (Acid Phosphatase Leukocyte No. 387, Sigma–Aldrich). Samples were counterstained for 10 min in haematoxylin solution and washed with water. Samples were assessed by bright-field optical microscopy (10× magnification, NA 0.3).

Immuofluorescence

Cells fixed (4% formaldehyde/PBS with 1% sucrose) at 37°C for 15 min. The samples were washed with PBS and a permeabilizing buffer (10.3 g of sucrose, 0.292 g of NaCl, 0.06 g of $MgCl_2$, 0.476 g of 4-(2-hydroxyethyl)-1-piperazineethanesulfonic acid (HEPES) buffer, 0.5 mL of Triton X, in 100 mL of water, pH 7.2) at 4°C for 5 min, then incubated at 37°C for 5 min in 1% bovine serum albumin (BSA)/PBS.This was followed by the addition of rhodamine-conjugated phalloidin (1:100 in 1% BSA/PBS, Invitrogen, UK) for 1 h (37°C). The samples were then washed in 0.5% Tween 20/PBS (37°C for 5 min). A final wash series followed prior to the addition of 4′,6-diamidino-2-phenylindole (DAPI) in mounting medium (Vectashield, Vector Laboratories, England, UK) and the samples were viewed using a fluorescence microscope (Zeiss Axiovert 200 M, 40× magnification, NA 0.5). For cell count osteoclasts were defined as cells greater than 30 μm in diameter, with 3 or greater nuclei and the presence of actin ring.

Atomic force microscopy

The ceramic utilised was biphasic consisting of a nanoscale grain; the grain being two sizes. Atomic force microscopy (AFM; JPK NanoWizard) was performed to yield quantitative data about our experimental ZTA surfaces such as microparticle size and roughness.

Results

SEM analysis of the patterned materials demonstrated successful micropatterning of the ZTA ceramic with approximately 30 μm diameter, 1.7 μm depth pits due to sintering shrinkage (Figure 1(a)). The nanocrystalised alumina and zirconia grain was also clearly visible with bright zirconia grains sitting on alumina grain boundaries (Figure 1(a)). AFM showed a range of sub-micrometre/nanometre scale features that the cells would be cultured on (ranging from

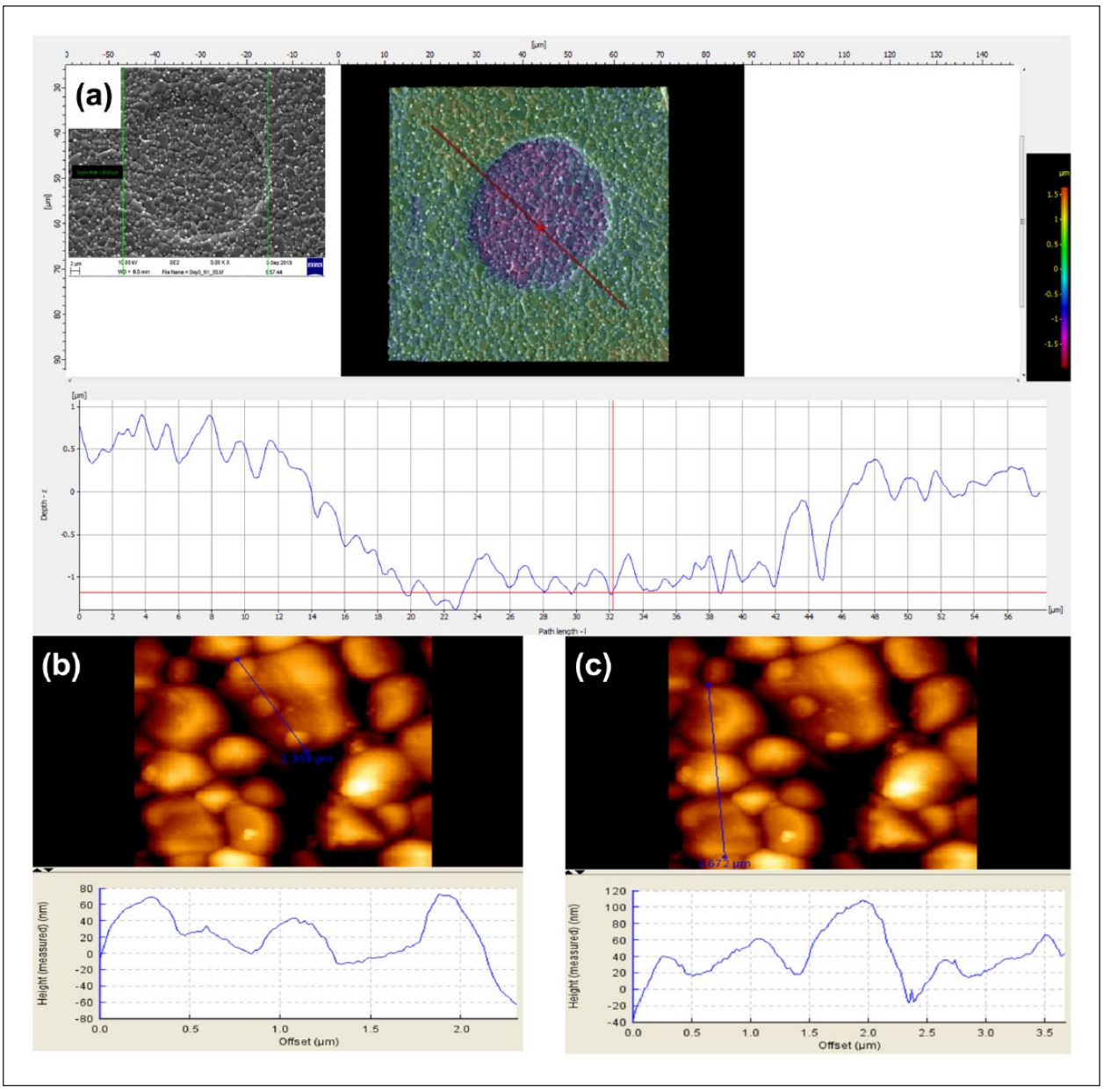

Figure 1. (a) AFM of the micropatterned materials. The pits in the imprinted ceramic have a mean diameter of 30 μm as shown by SEM. (b, c) AFM showed the particle diameters ranged from sub-micrometre/nanometre scale ((b), typically 500–700 nm diameter) to micrometre scale ((c), typically 1.5 μm in diameter).
AFM: atomic force microscopy; SEM: scanning electron microscopy.

0.5 to 1.5 μm in diameter, Figure 1(b) and (c)). The average roughness was 30.9 ± 9.3 nm. TRAP analysis after 28 days of culture showed many TRAP positive macrophages fusing into large, TRAP positive, osteoclasts. These were surrounded by TRAP-negative BMSC (Figure 2(a) and (b)). Fluorescence microscopy revealed the presence of multinucleated cells with distinct cortical actin rings typical of osteoclasts (Figure 2(c)). Furthermore, three-dimensional (3D) SEM imaging showed the presence of osteoclastic podosomes on some of the osteoclasts (Figure 2(d)).

Osteoclasts are formed from the fusing of macrophages in contact with bone. At early time points, one would expect to see mainly macrophages and BMSC, with BMSC being spread with fibroblastic morphology and macrophages being rounded, containing a small lamellae. Microscopy at 3 days demonstrated this to be the case on both flat control (Figure 3(a)) and the pitted substrates (Figure 3(e)). Macrophages were appeared to be interacting with the ceramic grain through filopodia formation (Figure 3(c) and (d)). This interaction was also seen clearly at longer time points (as shown in Figures 4 and 5) and

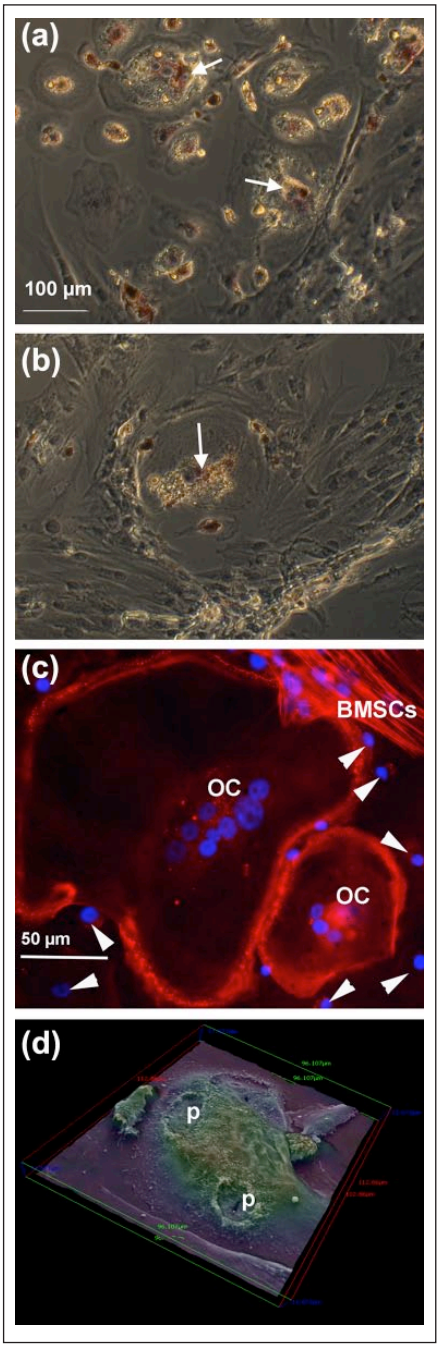

Figure 2. Immunofluorescence staining after 28 days of co-culture: (a, b) TRAP staining in BMSC and BMHC, derived from the same patient without media supplementation. (c) DAPI and actin fluorescence staining showing the presence of large multinucleated cells. Arrows illustrate TRAP positive cells, arrowheads indicate macrophage-like cells, OC indicates osteoclasts. (d) 3D SEM image showing podosome formation in cultured osteoclasts (p). These figures demonstrate ability of our co-culture to form osteoclasts and were performed on planar polycarbonate.
TRAP: tartrate-resistant acid phosphatase; BMSC: bone marrow–derived mesenchymal stromal cells; BMHC: bone marrow–derived haematopoietic cells; DAPI: 4′,6-diamidino-2-phenylindole; 3D: three-dimensional; SEM: scanning electron microscopy.

occasionally, much larger, osteoclast-like cells could be observed (Figure 3(a) and (b)). On the micropatterned surfaces, the cell response was markedly different. Less osteoclast-like cells were noted with more macrophaging or perhaps pre-osteoclastic cell formation. Macrophage-like cells could be seen overlapping pits, but did not appear to contact guide to the pit edges (Figure 3(f)).

By day 21, the osteoclastic cells could be more regularly seen on the planar control (Figure 4(a), (c) and (d)). There was some evidence of nascent bone nodules forming from groups of BMSC (Figure 4(b)) by day 14. On the pitted samples, however, there was little evidence of macrophage fusion to osteoclasts (Figure 4(e)). Rather, more macrophage-like cells were still visible. However, larger aggregates of BMSC forming bone nodules were frequently noted on the pitted surfaces at day 21 (Figure 4(f)–(h)).

At the longest time-point (day 28), osteoclast-like cells were visible across the planar surfaces and had strong interactions with the ceramic grains (Figure 5(a)–(d)). Podosomes were notable on some of the osteoclast membranes (Figure 5(c)). On the pitted surfaces, we observed very few osteoclast-like cells (Figure 5(e)), and rather pit bridging by macrophage-like cells was regularly noted (Figure 5(f) and (g)). The bridging cells were seen to be retracting over the pits, leaving retraction fibres (outset for Figure 5(f)) likely from where they had travelled from and interacting with the ceramic grain. Macrophage filopodia were also seen to interact with the grain, but as with days 3 and 21, not the pits (Figure 5(h)). Furthermore, sometimes macrophage-like cells were seen avoiding the pits (Figure 6(a)–(c)), interacting around them, but not into them.

Discussion

These results demonstrated a successful co-culture of BMSC and BMHC cell lineages with differentiation and maturation of cells towards those seen in normal human bone on both microtopography and control ceramics. In many places, nodular clusters of osteoblast-like cells were noted, derived from BMSC. This is encouraging as it demonstrates that there is bone forming potential on these surfaces, and that ceramic surfaces can support adhesion and differentiation of our BMSC/BMHC co-culture and ties in with data on pure osteoblast/osteoprogenitor cultures on similar shaped features in polymers.[16,17]

Osteointegration is fundamental for the success of biomedical implants. We have previously shown that microtopography can increase osteoblast adhesion and bone forming matrix in polymers and thus may improve implant osteointegration.[14] Ceramic materials are gaining popularity in arthroplasty due to their strength, wear properties and biocompatibility. However, there is a paucity of the literature regarding stem cell response to ceramic surface properties. Physical modification of ceramics is an attractive

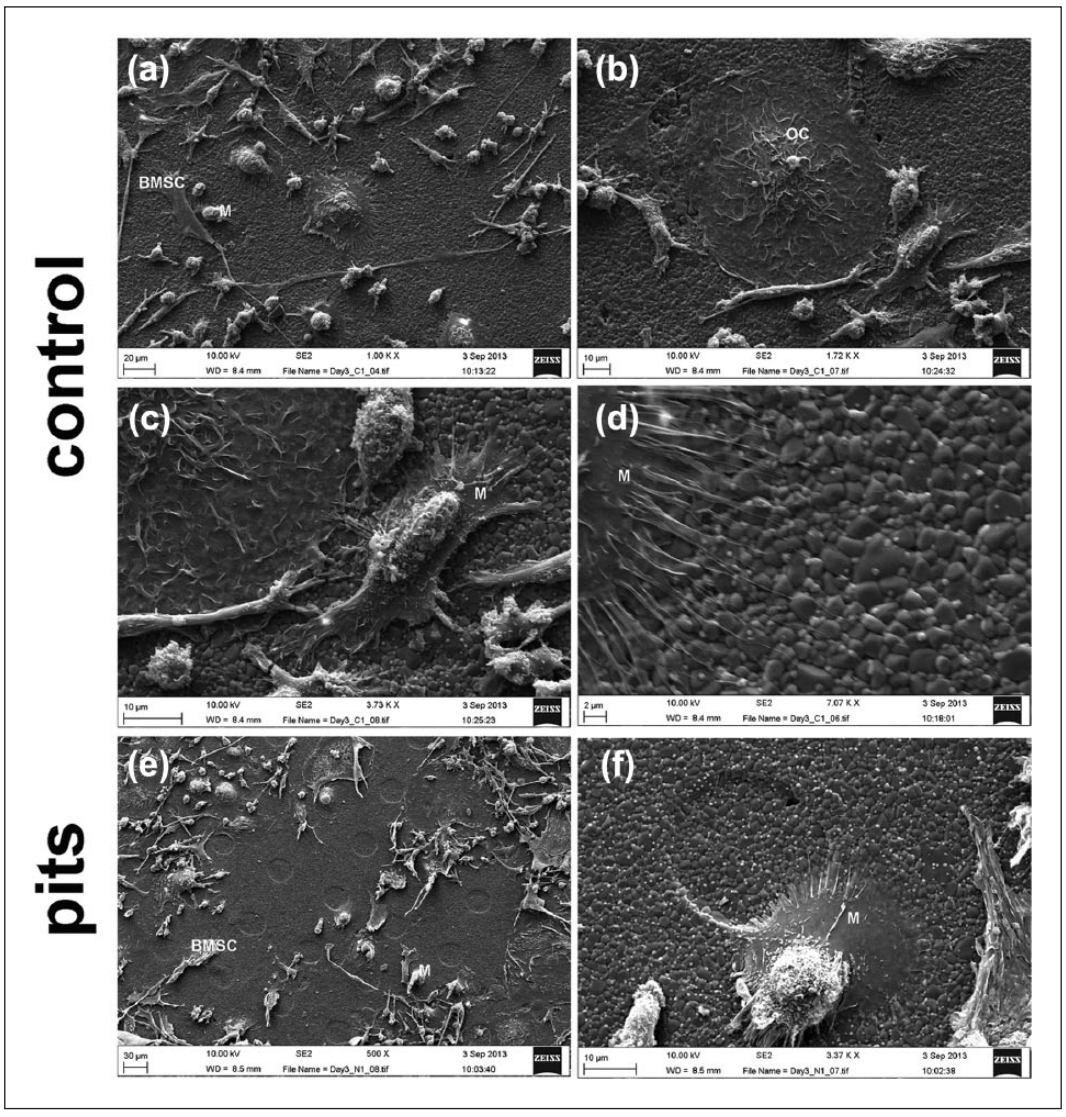

Figure 3. Scanning electron micrographs of BMHC and BMSC co-cultured on planar control and micropatterned ceramic test materials at day 3. Low magnification images of the co-cultures on planar (a) and patterned (e) substrates showing the presence of cells with macrophage (BMHC) and fibroblast (BMSC) morphologies. (b) OC observed on the planar surface. (c, d) BMHC with macrophage-like appearance (M) were regularly seen to interact with the nanotopographical detail of the ceramic grain with filopodia. (f) They also could be seen to interact with the lip of micropits.
BMHC: bone marrow–derived haematopoietic cells; BMSC: bone marrow–derived mesenchymal stromal cells; OC: osteoclastic cells.

method to increase osteointegration. However, ceramics are highly notch sensitive and any change in surface topography may have adverse consequence to their mechanical properties, especially fracture toughness. It is important to note that the fabrication of well-defined ceramic micropatterns smaller than 100 μm is technically challenging because of the inherent hardness and brittleness of ceramic materials.[30] Hence, we have previously examined the physical properties of this material to check that the pits do not affect its brittleness and physical properties. As micropatterning was carried out in the green (unsintered) state, any micro-cracks or notches were smoothed out during final sintering stage, which means they do not affect the physical properties compared to post-sintering roughening.[18] The ceramic pits showed good micropatterning fidelity but it is noted that nanopatterning of ceramics would be challenging due to the presence of ceramic grain. Our results indicate that microtopography can be used as a physical cue to modulate the BMSC's response to form bone.

In the field of osteogenesis, understanding the interaction between the host environment, containing an abundance of BMSC and BMHC, and biomaterials is of vital importance for producing implants with increased lifespan. Co-cultures are well recognised as a more accurate method of reproducing in vitro the environment into which biomaterials are implanted in vivo. Several other authors

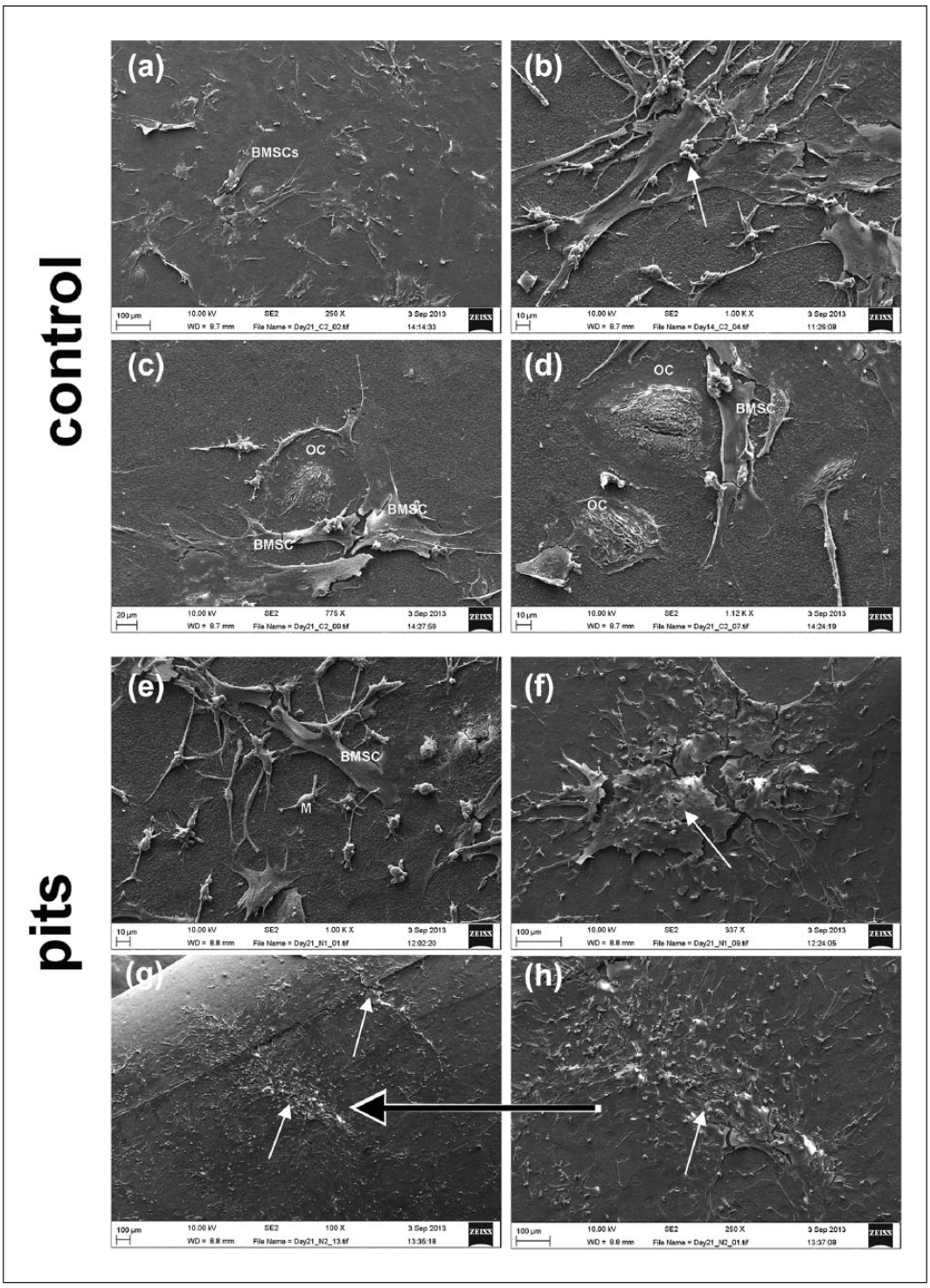

Figure 4. Scanning electron micrographs of BMHC and BMSC co-cultures at days 14 and 21. Low magnification images of the co-cultures on planar (a) and patterned (e) substrates showing the presence of cells with macrophage (BMHC) and fibroblast (BMSC) morphologies at day 21. (c, d) Large OC could be regularly observed on the planar controls. While nascent nodules (smaller white arrows) could occasionally be found on planar control at day 14 (b), these were larger and more prevalent on the micropatterned substrates (f–h). (h) Larger magnification of the nodule shown in (g).
BMHC: bone marrow–derived haematopoietic cells; BMSC: bone marrow–derived mesenchymal stromal cells; OC: osteoclastic cells.

report successful co-cultures of osteoblasts and osteoclasts, often using peripheral or murine derived monocytes, or using supplementation with RANKL and M-CSF to encourage osteoclast differentiation. We believe our method most closely represents the environment encountered by orthopaedic and dental implants as it utilises

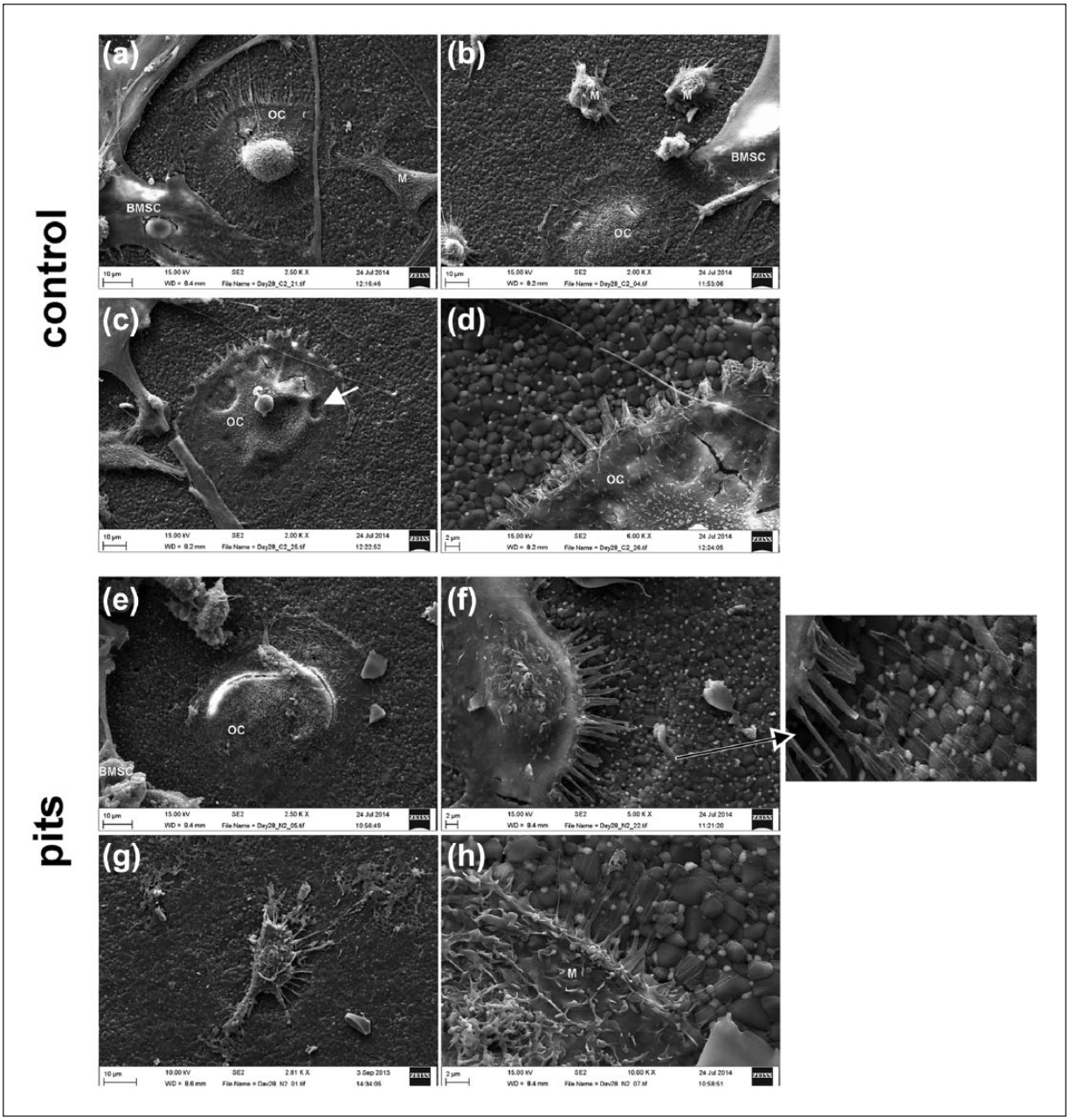

Figure 5. Scanning electron micrographs of the substrates at day 28. (a–d) Osteoclast-like cells visible across the planar surfaces showing interactions with ceramic grains. (d) Podosomes were visible (arrow) on some of the osteoclasts. (e) Few osteoclast-like cells with pit bridging by macrophage-like cells (f, g) The bridging cells retracting over the pits, leaving retraction fibres (outset in (f)). Macrophage filopodia were also seen to interact with the grain but not the pits (h).

human BMSC and BMHC directly obtained from the implant environment, cultured without the use of additional supplementation to encourage specific cell lineage differentiation. Our results demonstrate a viable co-culture of both osteoblastic and osteoclastic cells on ceramic materials validating this method.

Our results illustrate that the micropatterns do not increase osteoclastogenesis. In fact, they appeared to even reduce the formation of osteoclast-like cells compared to the planar control group. The fact that the macrophage-like cells appeared to change their morphology to avoid the pits is interesting to note (Figure 6(b)). In addition, the osteoclast-like cells were less frequently observed on the pitted substrates. We believe the explanation for this observation is that the pits resemble resorption lacunae, and the small osteoclast-like cells are perhaps fooled into thinking resorption has already occurred and therefore are not stimulated to fuse to

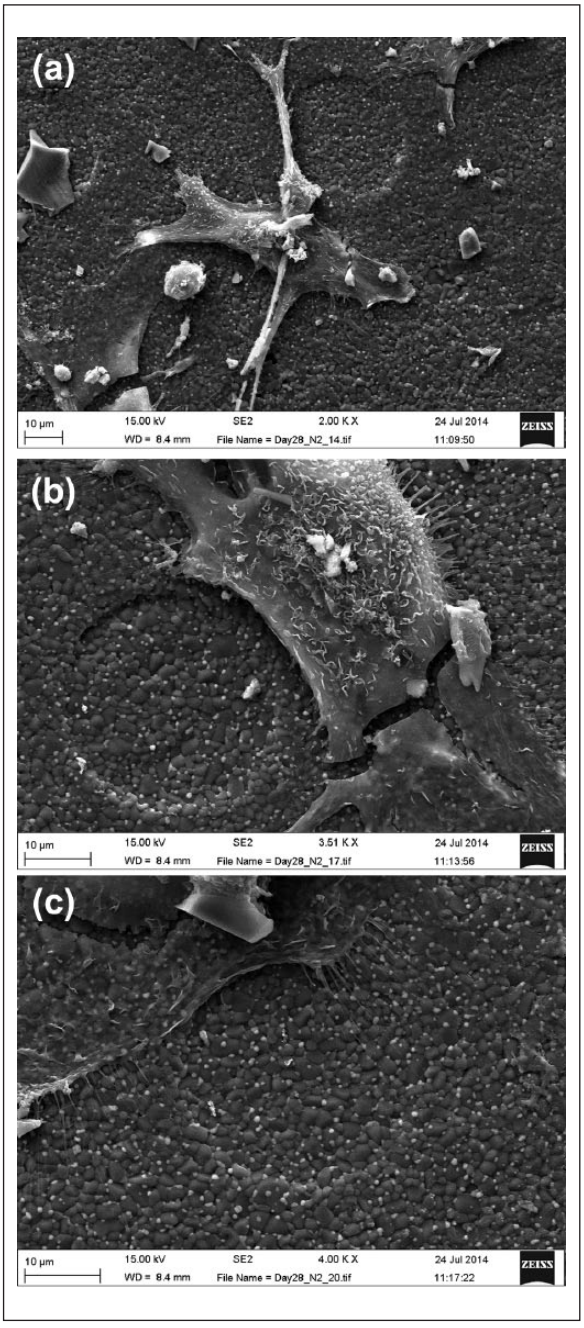

Figure 6. Scanning electron micrographs of the micropatterned substrates at day 28. Macrophage-like cells seen avoiding the pits (b), interacting around them, but not with them (a, c).

become mature osteoclasts, nor form sealing zones.[16] It is tempting to further speculate that the same lacunae-like features are osteoblast stimulatory, resembling the features they are primed to fill in vivo.[17] Thus, it is tempting to speculate that the pits may delay/reduce osteoclastogenesis while promoting osteoblastogenesis. Our future work will seek to establish a quantitative relationship and the underlying mechanisms.

Conclusion

We have developed a novel human BMSC and BMHC coculture, which has been successfully cultured on micropatterned ZTA ceramics. We believe this most accurately represents the osseous environment into which biomaterials are implanted and may be of interest to other researchers in this field. The cells responded to the topographical cues by clustering and filopodial sensing. These results suggest human BMSC are sensitive to micro features and are capable of forming bone nodules within 21 days of culture on the micropatterned surfaces. We further illustrate that micropatterned ZTA ceramics are specifically bioactive increasing bone nodule formation but appear to discourage osteoclastogenesis.

Acknowledgements

The authors thank Mrs Carol-Anne Smith for her help in the laboratory. The authors thank Mr Peter Chung, Ms Debra Chong and Ms Eleni Grigoriou for their help with the imaging. M.J.D. and R.M.D.M. are funded by grants from BBSRC, EPSRC and MRC.

Declaration of conflicting interests

The authors declare that there are no conflicts of interest.

Funding

This work was specifically funded by EPSRC grant EP/G048703/1.

References

1. Branemark R, Branemark PI, Rydevik B, et al. Osseointegration in skeletal reconstruction and rehabilitation: a review. *J Rehabil Res Dev* 2001; 38(2): 175–181.
2. Arvidson K, Abdallah BM, Applegate LA, et al. Bone regeneration and stem cells. *J Cell Mol Med* 2011; 15(4): 718–746.
3. Puleo DA and Nanci A. Understanding and controlling the bone-implant interface. *Biomaterials* 1999; 20(23–24): 2311–2321.
4. Purdue PE, Koulouvaris P, Nestor BJ, et al. The central role of wear debris in periprosthetic osteolysis. *HSS J* 2006; 2(2): 102–113.
5. Boyle WJ, Simonet WS and Lacey DL. Osteoclast differentiation and activation. *Nature* 2003; 423(6937): 337–342.
6. Rajpura A, Kendoff D and Board TN. The current state of bearing surfaces in total hip replacement. *Bone Joint J* 2014; 96-B(2): 147–156.
7. Oonishi H, Ueno M, Kim SC, et al. Ceramic versus cobalt-chrome femoral components; wear of polyethylene insert in total knee prosthesis. *J Arthroplasty* 2009; 24(3): 374–382.
8. Hamilton DW and Brunette DM. The effect of substratum topography on osteoblast adhesion mediated signal transduction and phosphorylation. *Biomaterials* 2007; 28: 1806–1809.
9. Stevens MM and George JH. Exploring and engineering the cell surface interface. *Science* 2005; 310(5751): 1135–1138.

10. Andersson A-S, Olsson P, Lidberg U, et al. The effects of continuous and discontinuous groove edges on cell shape and alignment. *Exp Cell Res* 2003; 288(1): 177–188.
11. Dalby MJ, Gadegaard N and Oreffo R. Harnessing nanotopography and integrin-matrix interactions to influence stem cell fate. *Nat Mater* 2014; 13(6): 558–569.
12. Clark P, Connolly P, Curtis AS, et al. Topographical control of cell behaviour. I. Simple step cues. *Development* 1987; 99(3): 439–448.
13. Dalby MJ, Riehle MO, Yarwood SJ, et al. Nucleus alignment and cell signaling in fibroblasts: response to a micro-grooved topography. *Exp Cell Res* 2003; 284(2): 274–282.
14. Wilkinson A, Hewitt RN, McNamara LE, et al. Biomimetic microtopography to enhance osteogenesis in vitro. *Acta Biomater* 2011; 7(7): 2919–2925.
15. Chen H, Song W, Zhou F, et al. The effect of surface microtopography of poly(dimethylsiloxane) on protein adsorption, platelet and cell adhesion. *Colloids Surf B Biointerfaces* 2009; 71(2): 275–281.
16. Dalby MJ, McCloy D, Robertson M, et al. Osteoprogenitor response to defined topographies with nanoscale depths. *Biomaterials* 2006; 27(8): 1306–1315.
17. Mata A, Hsu L, Capito R, et al. Micropatterning of bioactive self-assembling gels. *Soft Matter* 2009; 5(6): 1228–1236.
18. Anselme K and Bigerelle M. Topography effects of pure titanium substrates on human osteoblast long-term adhesion. *Acta Biomater* 2005; 1(2): 211–222.
19. Nadeem D, Sjostrom T, Wilkinson A, et al. Embossing of micropatterned ceramics and their cellular response. *J Biomed Mater Res A* 2013; 101: 3247–3255.
20. Bloemen V, De Vries TJ, Schoenmaker T, et al. Intercellular adhesion molecule-1 clusters during osteoclastogenesis. *Biochem Biophys Res Commun* 2009; 385: 640–645.
21. Greiner S, Kadow-Romacker A, Schmidmaier G, et al. Cocultures of osteoblasts and osteoclasts are influenced by local application of zoledronic acid incorporated in a poly(D,L-lactide) implant coating. *J Biomed Mater Res A* 2009; 91: 288–295.
22. Jones GL, Motta A, Marshall MJ, et al. Osteoblast: osteoclast co-cultures on silk fibroin, chitosan and PLLA films. *Biomaterials* 2009; 30: 5376–5384.
23. Nakagawa K, Abukawa H, Shin MY, et al. Osteoclastogenesis on tissue-engineered bone. *Tissue Eng* 2004; 10: 93–100.
24. Mbalaviele G, Jaiswal N, Meng A, et al. Human mesenchymal stem cells promote human osteoclast differentiation from CD34+ bone marrow hematopoietic progenitors. *Endocrinology* 1999; 140: 3736–3743.
25. Heinemann C, Heinemann S, Worch H, et al. Development of an osteoblast/osteoclast co-culture derived by human bone marrow stromal cells and human monocytes for biomaterials testing. *Eur Cell Mater* 2011; 25(21): 80–93.
26. Haynesworth SE, Baber MA and Caplan AI. Cytokine expression by human marrow-derived mesenchymal progenitor cells in vitro: effects of dexamethasone and IL-1 alpha. *J Cell Physiol* 1996; 166: 585–592.
27. Lim JH, Park EC, Lee SY, et al. Fabrication of Ni metal mask by electroforming process using wetting agents. *J Electronic Mater* 2007; 36(11): 1510–1515.
28. Su B and Button TW. A comparative study of viscous polymer processed ceramics based on aqueous and non-aqueous binder systems. *J Mater Process Technol* 2009; 209(1): 153–157.
29. Young PS, Tsimbouri PM, Gadegaard N, et al. Osteoclastogenesis/osteoblastogenesis using human bone marrow derived co-cultures on nanotopographical polymer surfaces. *Nanomedicine*, in press.
30. Su B, Zhang D and Button TW. Micropatterning of 3D ceramic microstructures. *J Mater Sci* 2002; 37: 3123–3126.